

PACS numbers: 42.72.Bj; 52.80.Yr; 85.40.Hp
DOI: 10.1070/QE2009v039n10ABEH014028

Laser-induced extreme UV radiation sources for manufacturing next-generation integrated circuits

V.M. Borisov, A.Yu. Vinokhodov, A.S. Ivanov, Yu.B. Kiryukhin,
V.A. Mishchenko, A.V. Prokof'ev, O.B. Khristoforov

***Abstract*. The development of high-power discharge sources emitting in the 13.5 ± 0.135-nm spectral band is of current interest because they are promising for applications in industrial EUV (extreme ultraviolet) lithography for manufacturing integrated circuits according to technological precision standards of 22 nm and smaller. The parameters of EUV sources based on a laser-induced discharge in tin vapours between rotating disc electrodes are investigated. The properties of the discharge initiation by laser radiation at different wavelengths are established and the laser pulse parameters providing the maximum energy characteristics of the EUV source are determined. The EUV source developed in the study emits an average power of 276 W in the 13.5 ± 0.135-nm spectral band on conversion to the solid angle 2π sr in the stationary regime at a pulse repetition rate of 3000 Hz.**

Keywords: *EUV source, EUV lithography, plasma, discharge, lasers.*

1. Introduction

The rapid development of microelectronics in last decades is related to advances achieved in the reduction of the distance Δx between the elements of microcircuits fabricated with the help of photolithography. According to the Rayleigh criterion, $\Delta x = k\lambda/\mathrm{NA}$, where k is a coefficient close to unity; λ is the radiation wavelength; $\mathrm{NA} = n \sin\alpha$ is the numerical aperture of an objective; and n is the refractive index of a medium. Thus, the spatial resolution of the lithographic equipment can be improved by decreasing the radiation wavelength, increasing the numerical aperture of the objective (by increasing the aperture angle α or using an immersion liquid with $n > 1$), and decreasing the coefficient k.

At present integrated circuits are fabricated by using, as a rule, lithographs in which a UV radiation source is a 193-nm excimer ArF laser. It is assumed that the use of phase masks and (or) immersion liquids in projection lithography at a wavelength of 193 nm will provide the spatial resolution up to $\Delta x \approx 32 - 22$ nm [1]. To obtain better resolution, it is necessary to use shorter-wavelength radiation. However, in this case the problem of the absence of transparent materials useful for the construction of optical systems appears. This problem can be solved by using a projection system based on reflecting mirrors. Radiation at a wavelength of 13.5 nm in the EUV (extreme ultraviolet) region is the most optimal for using in a next-generation lithography [2]. The choice of this wavelength is elated to the fabrication of Bragg MoSi mirrors with a high reflectance ($\sim 70\,\%$) in a narrow spectral band at 13.5 nm with the relative width $\Delta\lambda/\lambda = 2\,\%$ for a system of several MoSi mirrors.

According to the economically substantiated productivity of an industrial EUV scanner (~ 100 silicon substrates of diameter 300 mm per hour [2]), the required EUV power at 13.5 nm in the band of relative width $\Delta\lambda/\lambda = 2\,\%$ should be 2–3 kW on conversion to the solid angle 2π sr. To provide the efficient collection and transport of EUV radiation on a substrate with the help of optical systems developed at present, the characteristic linear size of the emitting plasma volume should not exceed 1 mm. The resource of the source and collecting optics should be $\sim 10^{11}$ pulses [2]. This means that optical elements should be reliably protected from any contaminations produced by the source. The requirement of a high average EUV power in conjunction with a small emitting plasma volume and a large operating life makes the development of such a radiation source one of the key conditions for the realisation of highly productive EUV lithography.

Plasma sources can be efficiently used in EUV lithography because the high-temperature plasma of a number of elements (Xe, Sn, Li) exhibits intense emission at a wavelength of 13.5 nm. Such plasma can be obtained either by focusing high-power laser radiation on a target or in a discharge [3]. In the latter case, the electric energy stored in a capacitor bank is directly transformed to the plasma energy. The use of a classical Z-pinch in Xe as a radiation source for EUV lithography was first proposed in [4]. Several EUV radiation sources based on a modified Z-pinch in Xe and emitting up to ~ 100 W $(2\pi \text{ sr})^{-1}$ have been fabricated by researchers at the SRC RF TRINITI in cooperation with XTREME Technologies GmbH (Germany) in 2000–2004 [5]. Other types of discharges in Xe such as a plasma focus [6], a hollow-cathode discharge [7], and a capillary discharge [8] have also been investigated as EUV radiation sources. All these discharges have an axially symmetric electrode

V.M. Borisov, A.Yu. Vinokhodov, A.S. Ivanov, Yu.B. Kiryukhin, V.A. Mishchenko, A.V. Prokof'ev, O.B. Khristophorov State Research Center of the Russian Federation, Troitsk Institute for Innovation and Fusion Research (SRC RF TRINITI), 142190 Troitsk, Moscow region, Russia; e-mail: borisov@triniti.ru, khristofor@triniti.ru

Received 17 December 2008; revision received 15 April 2009
Kvantovaya Elektronika **39** (10) 967–972 (2009)
Translated by M.N. Sapozhnikov

system with a small (no more than 10 cm^2) working electrode surface, which leads to their strong erosion due to high electric and thermal loads. The electrode erosion rate under typical discharge conditions of the Z-pinch formation in Xe is $10^{-7} - 10^{-8}$ g $pulse^{-1}$ [5]. A strong erosion of electrodes prevents the achievement of the operating life of the EUV radiation source required for an industrial lithograph because the emitting plasma volume and EUV radiation power change with changing the electrode geometry caused by erosion. At a power of 10 kW supplied to the discharge, all these parameters are preserved only during $\sim 1.5 \times 10^8$ pulses [5].

Another serious obstacle for using a Z-pinch discharge in Xe as a EUV radiation source for industrial lithographs is its low efficiency. The conversion efficiency of the EUV radiation source is usually defined as the ratio of the EUV energy, emitted in a narrow spectral band $\Delta\lambda/\lambda = 2\,\%$ at 13.5 nm within a solid angle of 2π sr, to the electric energy stored in a capacitor bank. The typical conversion efficiency of a EUV radiation source based on a discharge in Xe is 0.5 % [3, 5–8]. A considerably higher efficiency ($\sim 2\,\%$) is achieved in tin plasmas [7, 9, 10].

The aim of this paper is to study the possibility of creation of a radiation source for industrial EUV lithography based on a discharge in tin vapours initiated by a laser between rotating disc electrodes (RDEs).

2. Experimental EUV radiation source with rotating disc electrodes

Figure 1 shows schematically the design of a EUV radiation source in which disc cathode (*1*) and anode (*2*) fastened with insulator (*3*) are rotated with the help of electric motor (*4*) on a common shaft. Pulse-charged capacitor bank (*5*) located between two disc electrodes and connected with them with a minimal inductance is rotated together with electrodes. Anode and cathode discs have channels for circulation of a cooling liquid supplied by means of cooling system (*6*) through the shaft. The capacitor bank is charged with the help of pulsed power supply (*7*) through sliding contacts (*8*). High-power turbomolecular pump (*9*) provides a working pressure of ~ 0.1 Pa in chamber (*10*), which eliminates parasitic breakdowns between RDEs.

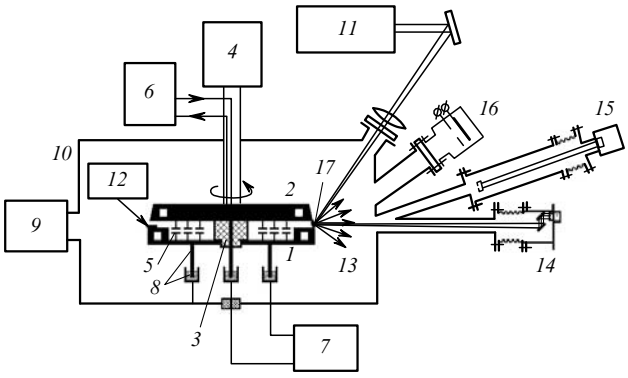

Figure 1. Scheme of an experimental EUV source with the laser-initiated discharge in tin vapours between RDEs: (*1*) cathode; (*2*) anode; (*3*) insulator; (*4*) electric motor; (*5*) capacitor bank; (*6*) cooling system; (*7*) pulsed power supply; (*8*) sliding contacts; (*9*) turbomolecular pump; (*10*) vacuum chamber; (*11*) laser; (*12*) tin regeneration system; (*13*) EUV radiation; (*14*) EUV energy and power meter; (*15*) system for recording the image of plasma emitting in the EUV region; (*16*) Faraday cylinder; (*17*) discharge plasma.

A discharge between RDEs appears only after the action of the focused beam from laser (*11*) on the edge of one of the discs (usually cathode) covered with a tin layer. The laser pulse produces tin plasma and vapours in the interelectrode space due to ablation, thereby initiating a breakdown. Compared to coaxially symmetric electrode systems used in [5–8], the working surface of RDEs is increased, and the metal from which electrodes are fabricated is protected from erosion by a tin layer, which forms the plasma. A large enough surface of cooling channels provides the efficient removal of heat released in electrodes.

Note that the concept of a radiation source shown in Fig. 1 was first presented in our report [11] at the EUV Source Workshop in Antwerp in 2003.

System (*12*) provides the supply of tin on the cathode surface and its levelling. In one of the versions of the radiation source, liquid tin was supplied to the working electrode region through a porous structure from the internal circular cavity of electrodes under the action of capillary and centrifugal forces.

The EUV radiation energy and power (*13*) emitted by the discharge plasma in the required spectral range were measured with calibrated energy and power meter (*14*) consisting of a 0.2-μm-thick Zr filter, which absorbed visible and UV radiation, two MoSi mirrors providing the relative transmission bandwidth of 2 % at 13.5 nm, and an AXUV-100G (IRD Inc.) photodiode whose output signals were recorded with an oscilloscope. The image of the plasma emitting in the EUV range was recorded by system (*15*) containing a camera obscura with a hole of diameter 100-μm, a CCD array, and a Zr filter. The ion current was measured with Faraday cylinder (*16*). The discharge current and voltage were measured by means of a standard rated Rogowski loop and a high-voltage divider.

Although the walls of a vacuum chamber were water-cooled, the temperature of flanges began to increase when the electric power P supplied to the plasma exceeded 16 kW, which could result in the chamber seal failure. For this reason, long-term (stationary) experiments were performed for $P < 16$ kW. The discharge was initiated in experiments by KrF, XeF, Nd : YAG, or CO_2 lasers.

3. Characteristics and conditions of the optimal energy supply into a discharge

The EUV emission spectrum of a discharge of the type of a vacuum spark in tin vapours consists of the line spectra of highly ionised tin atoms (from SnVIII to SnXIII) (see, for example, [12]). To achieve the maximum emission intensity at 13.5 nm, the electron temperature should be ~ 30 eV [1, 3, 9]. A plasma with such electron temperature can be obtained in a pinch discharge, which is characterised by the compression and heating of a plasma shell under the action of the magnetic field B of the discharge current. The discharge pinching occurs when the pressure $B^2/2\mu_0$ (μ_0 is the magnetic constant) produced by the magnetic field exceeds the pressure of the tin plasma. The state of the art in the studies of pinching effects in a vacuum spark as described in detail in [9].

Figure 2 presents typical oscillograms characterising processes in a discharge in tin vapours produced by

$\sim$ 8-J laser pulses. Laser pulse (*1*) near the moment of the achievement of the maximum voltage (*2*) produces the initial plasma cloud on the cathode, which expands and closes the interelectrode gap. As a result, within $\sim$ 120 ns after the laser pulse, voltage (*2*) begins to decrease sharply and noticeable discharge current (*3*) appears, and after another 40 ns, when discharge current (*3*) increases up to $\sim$ 12 kA, EUV emission pulse (*4*) appears. The shape of this pulse demonstrates that pinching conditions appear several times during the discharge.

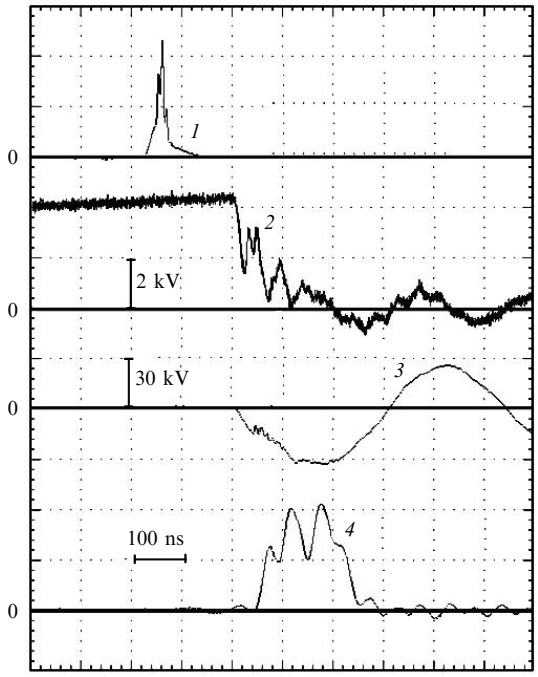

Figure 2. Oscillograms of a laser pulse (*1*), discharge voltage (*2*) and current (*3*), and a EUV pulse (*4*).

Note than under discharge excitation conditions presented in Fig. 2, the rate of increase in the discharge current dI/dt before the generation of the EUV pulse is approximately equal to 0.4×10^{12} A s^{-1}. It was shown experimentally in [13] that this rate is optimal for obtaining plasma parameters providing the maximum EUV emission intensity in the spectral range 13.5 ± 0.135 nm.

The maximum efficiency of the EUV radiation source achieved for $dI/dt \approx 0.4 \times 10^{12}$ A s^{-1} almost did not change during variations of parameters C, U, and L of the discharge excitation circuit. However, because $dI/dt \sim U/L$, to provide the optimal values of dI/dt with increasing the inductance L, it is necessary to increase the voltage U applied to capacitors connected with electrodes. This leads to the inefficient supply of energy to the discharge, when the energy remained in capacitors after the first half-period of the discharge current, which then uselessly dissipates in the discharge, can amount up to 50 % of the electric energy initially accumulated in capacitors.

The dependence of the conversion efficiency of the source on the electric energy E stored in the capacitor bank is presented in Fig. 3. The energy E was varied by changing the charging voltage at the pulse repetition rate $f = 100$ Hz. One can see from Fig. 3 that the conversion

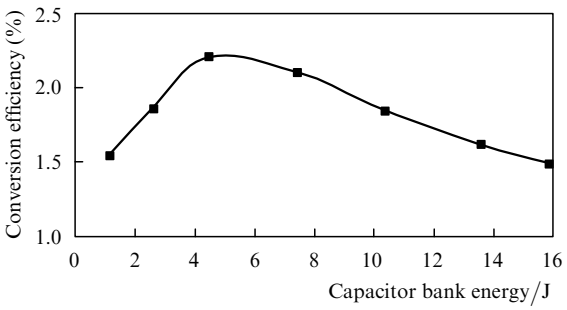

Figure 3. Dependence of the EUV source efficiency on the energy stored in a capacitor bank.

efficiency of the source is no less than 2 % for the stored energy from 3 to 9 J.

The energy remained in capacitors after the first half-period of the discharge current can be in principle transferred to the pulsed power supply for using in the next charging pulse. In this connection of interest is also the intrinsic efficiency η of conversion of the electric energy supplied to the discharge during the first half-period of the discharge current to the EUV radiation energy. The values of η in our experiments (for $f = 100$ Hz) were between 2.5 % and 3.0% when the energy supplied during the first half-period was varied from 2 to 6 J.

4. Characteristics of the laser initiation of a discharge

Our experiments showed that the discharge properties and conversion efficiency depend considerably on the conditions of laser initiation of the discharge. The laser initiation of the discharge in the EUV source was investigated by using different lasers with basic parameters presented in Table 1.

Table 1. Parameters of lasers used for initiating a discharge in a EUV source.

Laser	λ/μm	τ/ns	I_{max}/W cm^{-2}	E_{max}/mJ
KrF	0.248	12	2.2×10^9	60
XeF	0.351	6	8×10^8	30
Nd : YAG	1.06	30	10^9	75
Nd : YAG	1.06	8	1.3×10^{10}*	38*
			6×10^{9}**	17**
CO_2	10.6	100	2.7×10^8	250

Notes: λ is wavelength; τ is pulse FWHM; I_{max} is maximum radiation intensity in the focal spot; E_{max} is maximum energy at $f = 1$ (*) and 3 kHz (**).

It was found in experiments that the key parameter of a laser pulse is the laser power density q in the focal spot on the electrode surface. This is illustrated by the dependences of the conversion efficiency on q for different lasers (Fig. 4a).

Experiments performed in the study have led to the following conclusions:

(i) The laser power density q in the focal spot is the critical parameter for generation of EUV radiation.

(ii) The laser initiation of the discharge is possible only when q exceeds a certain critical value depending on the laser wavelength.

(iii) The dependence of the conversion efficiency on q saturates.

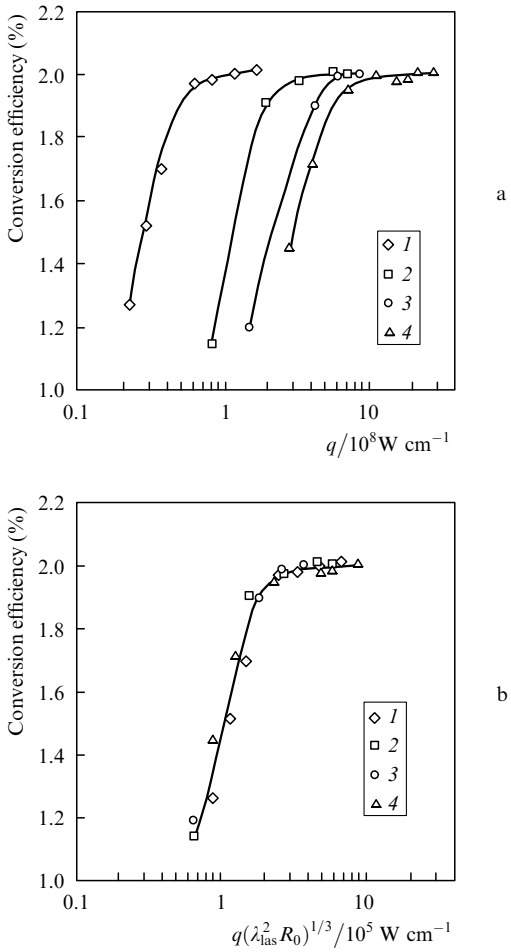

Figure 4. Dependences of the EUV source efficiency on the laser power density q (a) and parameter $q(\lambda_{las}^2 R_0)^{1/3}$ (b) for a 10.6-μm CO_2 laser and the focal spot size $S \approx 0.55 \times 0.64$ mm (*1*), a 1.06-μm Nd : YAG laser and $S \approx 0.48 \times 48$ mm (*2*), a 0.351-μm XeF laser and $S \approx 0.35 \times 1.2$ mm (*3*) and a 0.248-μm KrF laser and $S \approx 0.36 \times 0.61$ mm (*4*).

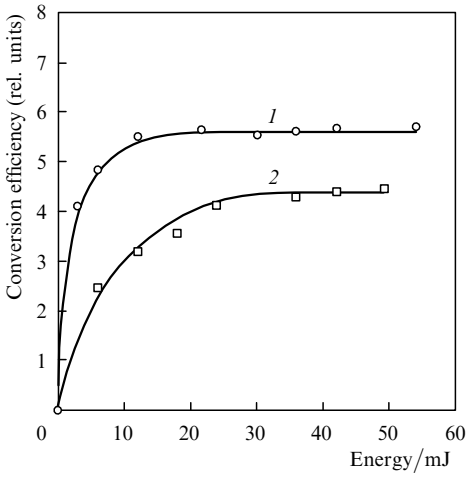

Figure 5. Dependences of the EUV source efficiency on the KrF laser energy for interelectrode distances 3 (*1*) and 6 mm (*2*).

(iv) The increase in the laser wavelength reduces the laser power density q_{th} at which saturation occurs. Thus, according to Fig. 4a, the CO_2 laser power density at which the conversion efficiency saturates is close to 10^8 W cm^{-2}, whereas for KrF laser it exceeds 10^9 W cm^{-2}.

It was shown in [13] that the electric conduction σ of the laser plasma in which the discharge current flows depends on the laser wavelength λ_{las} and the characteristic size R_0 of the focal spot as $\sigma \sim (q^2 \lambda_{las}^2 R_0)^{1/3}$. Along with the dependence on q (Fig. 4a), we also considered the dependence of the EUV source efficiency on the parameter $q(\lambda_{las}^2 R_0)^{1/3}$ (Fig. 4b). One can see from Fig. 4 that the data obtained for different lasers are well described by the same dependence of the EUV source efficiency on this parameter.

The results presented in Fig. 4 were obtained for the interelectrode distance of 3 mm. Figure 5 shows that the EUV source efficiency decreases with increasing the discharge gap from 3 mm [curve (*1*)] to 6 mm [curve (*2*)], which is explained by the increase in the discharge channel length and the redistribution of the energy supplied to the discharge between regions of the discharge emitting in the EUV range with different efficiencies. As the interelectrode distance was increased, the maximum source efficiency was achieved at higher laser energies (Fig. 5) and, correspondingly, at larger q, which can be explained by the decrease in the temperature of expanding laser plasma and the decrease in its electric conduction.

The value of q at which the maximum source efficiency is achieved is determined by the parameters of the energy supply into the discharge. Thus, the study of a RDE source showed that the maximum (~ 1 %) of the dependence of the conversion efficiency on q was achieved at the power density of a Nd : YAG laser of $\sim 9 \times 10^9$ W cm^{-2} [14]. This value is 30 times greater than $q \approx 3 \times 10^8$ W cm^{-2} [curve (*2*) in Fig. 4a] which provides the maximum efficiency (~ 2 %) of the source studied in our paper. Such a considerable discrepancy is explained by the fact that the inductance of the discharge circuit of the source in [14] was not small enough. As a result, the growth rate of current in this source was several times lower than that in Fig. 2, and the delay of the EUV pulse with respect to the initiating laser pulse exceeded 300 ns. During this time (according to the measurements of the dynamics of the electron density n_e in the laser plasma), the concentration of the laser plasma in the discharge pinching region decreases by many times due to plasma expansion. For this and other reasons, to achieve the maximum EUV emission intensity of the discharge plasma with not high enough values of dI/dt, much higher concentrations of the laser plasma and, hence, higher values of q are required.

5. Parameters of a radiation source in the stationary regime with a high pulse repetition rate

Figure 6 shows the EUV radiation intensity distribution in the discharge gap between rotating electrodes obtained with the help of a camera obscure. One can see that the discharge region from which the main part of the EUV energy is emitted is located near a cathode on which laser initiation is performed. The intense emission near the cathode is produced by a dense high-temperature plasma formed in a micropinch. The weaker emission observed near the opposite electrode (anode) appears due to the bombardment of the anode by electron fluxes and the interaction of cumulative jets of the high-temperature plasma with the near-anode plasma. The enhancement of EUV emission in the near-anode region occurs usually in the stationary regime and leads to a decrease in the

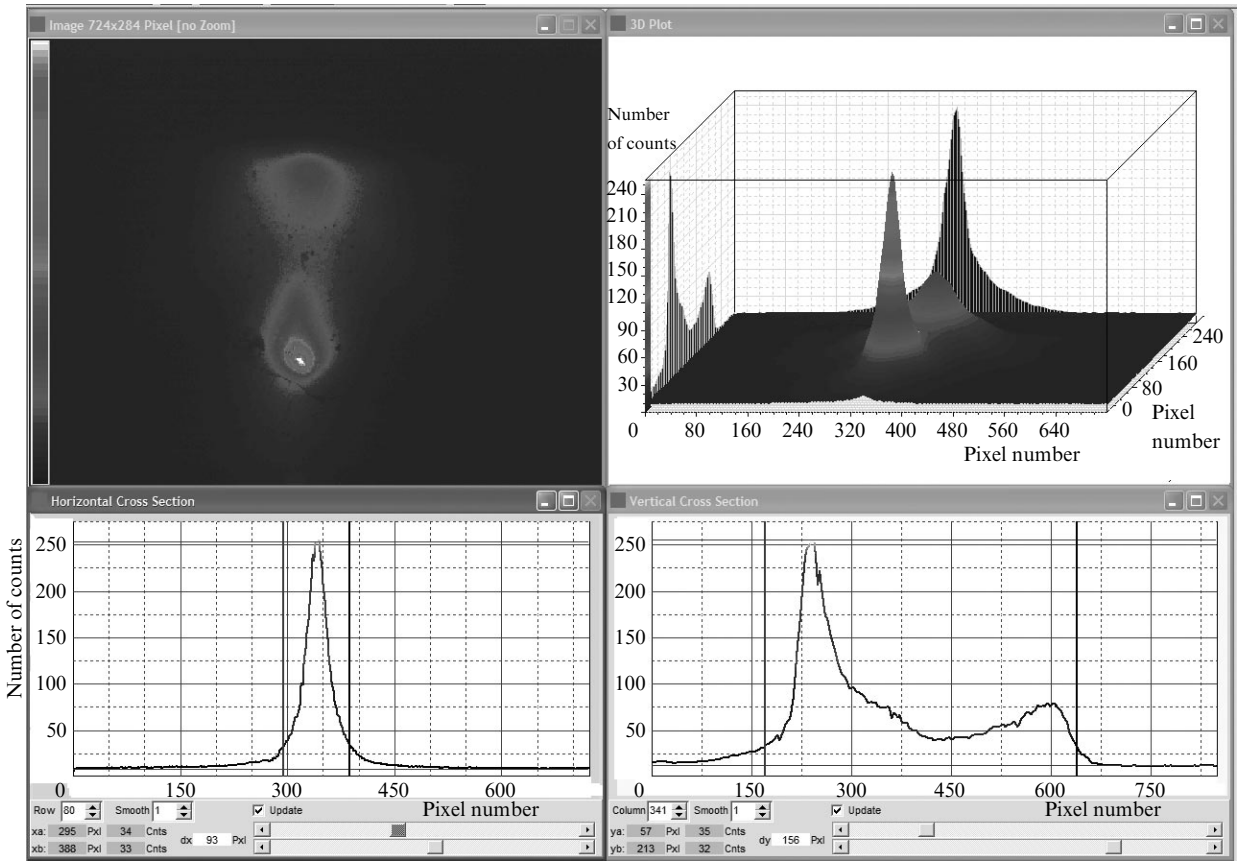

Figure 6. Image of plasma emitting in the EUV range (a) and the EUV radiation intensity profiles at the 18th minute of operation for $E = 9.9$ J and $f = 2$ kHz: 3D (b), horizontal (c), and vertical (d).

intensity of EUV emission from the near-cathode region and a decrease in the conversion efficiency.

Experiments performed in the stationary source operation regime showed that, when a 248-nm KrF laser was used, the EUV energy in a pulse decreased for $f > 2$ kHz. We explain this effect by the attenuation of initiating laser radiation incident on the cathode due to accumulation of tin vapours in the discharge zone and strong, proportional to $1/\lambda_{las}^4$, scattering of UV laser radiation. By using a longer laser wavelength (351-nm XeF laser), it was possible to perform the operation of the source at $f = 3$ kHz, by retaining the EUV pulse energy and the power $P =$ 16 kW supplied to te discharge in the stationary regime (for three hours). The sequences of the peak voltages and EUV signals for the source operating in the stationary regime at $f = 3$ kHz are presented in Fig. 7. The output EUV radiation power in the 13.5 ± 0.135-nm spectral band measured within the solid angle 2π sr was 276 W for the efficiency $\eta = 1.76\,\%$ and $2.24\,\%$.

The results obtained for the source in the stationary regime upon initiating the discharge by a Nd : YAG laser for $f = 3$ kHz are close to these obtained with a XeF laser (Fig. 7). According to our estimates, by using high-power Nd : YAG lasers, it is possible to increase the EUV power of the source by increasing f up to a few tens of kilohertz.

6. Conclusions

The optimal conditions for initiating the discharge and supplying energy to it found in the study allowed us obtain

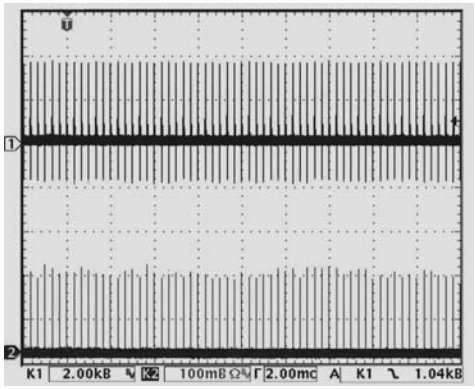

Figure 7. Sequences of the peak discharge voltages (2 kV div^{-1}) and the 13.5 ± 0.135-nm EUV radiation signals (0.52 mJ mV^{-1}) within the solid angle 2π sr in the stationary source operation regime at $f = 3$ kHz.

the long-term stationary operation regime of the source with the average EUV radiation power 276 W $(2\pi\ \text{sr})^{-1}$ in the spectral band 13.5 ± 0.135 nm for $f = 3$ kHz and the intrinsic efficiency $\eta \approx 2.2\,\%$.

It is interesting to compare the results presented in the paper with the recent results of other research groups involved in the development of sources with rotating disc electrodes. Thus, the authors of [15] obtained 170 W$\times$ $(2\pi\ \text{sr})^{-1}$ of EUV power in the stationary regime for $\eta = 2\,\%$ and $f = 5$ kHz. The resource of the source was $\sim 10^{11}$ pulses, which is required for industrial UUV lithography. In [14], ~ 580 W $(2\pi\ \text{sr})^{-1}$ was obtained in a short

train of EUV pulses for $\eta = 0.6\,\%$ and $f = 20$ kHz. The results obtained in [14, 15] and our paper demonstrate that further studies devoted to the development of discharge sources for industrial EUV lithography are promising.

Note that due to the limited volume of the paper, we did not discuss the important problem of generation of atoms, ions, and tin drops (so-called debris) from the discharge, which contaminate optical elements in the absence of protection. We plant to report the study on the elimination of debris elsewhere.

Acknowledgements. This work was supported by the Russian Foundation for Basic Research (Grant No. 08-08-00672a) and XTREME Technologies GmBH (ISTC Project No. 3599r).

References

1. Seisyan R. *Zh. Tekh. Fiz.*, **75**, 1 (2005).
2. Ota K. et al., in *EUV Source for Lithography*. Ed. by V. Bakshi (Bellingham, Wash.: SPIE Press, 2006) p. 3.
3. Jonkers J. *Plasma Sources Sci. Technol.*, **15**, 8 (2006).
4. McGeoch M. *Appl. Opt.*, **37**, 1651 (1998).
5. Borisov V. et al., in *EUV Source for Lithography*. Ed. by V. Bakshi (Bellingham, Wash.: SPIE Press, 2006) p. 477.
6. Fomenkov I. et al., in *EUV Source for Lithography*. Ed. by V. Bakshi, Bellingham, Wash.: SPIE Press, 2006) p. 373.
7. Pankert J. et al., in *EUV Source for Lithography*. Ed. by V. Bakshi (Bellingham, Wash.: SPIE Press, 2006) p. 395.
8. Teramoto Yu. et al., in *EUV Source for Lithography*. Ed. by V. Bakshi (Bellingham, Wash.: SPIE Press, 2006) p. 505.
9. Koshelev K. et al., in *EUV Source for Lithography*. Ed. by V. Bakshi (Bellingham, Wash.: SPIE Press, 2006) p. 175.
10. Borisov V. et al. *J. Phys. D: Appl. Phys.*, **37**, 3254 (2004).
11. Borisov V. et al. *EUV Source Workshop* (Antwerp, 2003), see www.sematech.org.
12. Tolsikhina Yu. et al., in *EUV Source for Lithography*. Ed. by V. Bakshi (Bellingham, Wash.: SPIE Press, 2006) p. 113.
13. Ivanov A.S. *Cand. Diss.* (Troitsk, SRC RF TRINITI, 2008).
14. Yokoyama T. et al. *Proc. SPIE Int. Soc. Opt. Eng.*, **7271**, 727139-1 (2009).
15. Corthout M. et al. *Proc. SPIE Int. Soc. Opt. Eng.*, **6921**, 69210V-1 (2008).